Cancer Research

Preclinical Characterization of BET Family Bromodomain Inhibitor ABBV-075 Suggests Combination Therapeutic Strategies

Mai H. Bui, Xiaoyu Lin, Daniel H. Albert, Leiming Li, Lloyd T. Lam, Emily J. Faivre, Scott E. Warder, Xiaoli Huang, Denise Wilcox, Cherrie K. Donawho, George S. Sheppard, Le Wang, Steve Fidanze, John K. Pratt, Dachun Liu, Lisa Hasvold, Tamar Uziel, Xin Lu, Fred Kohlhapp, Guowei Fang, Steven W. Elmore, Saul H. Rosenberg, Keith F. McDaniel, Warren M. Kati, and Yu Shen

Abstract

ABBV-075 is a potent and selective BET family bromodomain inhibitor that recently entered phase I clinical trials. Comprehensive preclinical characterization of ABBV-075 demonstrated broad activity across cell lines and tumor models, representing a variety of hematologic malignancies and solid tumor indications. In most cancer cell lines derived from solid tumors, ABBV-075 triggers prominent G_1 cell-cycle arrest without extensive apoptosis. In this study, we show that ABBV-075 efficiently triggers apoptosis in acute myeloid leukemia (AML), non-Hodgkin lymphoma, and multiple myeloma cells. Apoptosis induced by ABBV-075 was mediated in part by modulation of the intrinsic apoptotic pathway, exhibiting synergy with the BCL-2 inhibitor venetoclax in preclinical models of AML. In germinal center diffuse large B-cell lymphoma, BCL-2 levels or venetoclax sensitivity predicted the apoptotic response to ABBV-075 treatment. *In vivo* combination studies uncovered surprising benefits of low doses of ABBV-075 coupled with bortezomib and azacitidine treatment, despite the lack of *in vitro* synergy between ABBV-075 and these agents. The *in vitro*/*in vivo* activities of ABBV-075 described here may serve as a useful reference to guide the development of ABBV-075 and other BET family inhibitors for cancer therapy. *Cancer Res; 77(11); 2976–89. ©2017 AACR.*

Introduction

Reversible lysine acetylation has emerged as a central regulatory mechanism for chromosome remodeling, gene transcription, and other biological processes (1, 2). The BET family (BRD2, BRD3, BRD4, and BRDT) are bromdomain-containing proteins that interact with acetylated histone tails and play important roles in transcription regulation (3, 4). Among the BET family members, BRDT is primarily expressed in testis and ovary with a putative role in germ cell maturation (5). BRD2, BRD3, and BRD4 are ubiquitously expressed and reportedly interact with acetylated histone tails to regulate transcription through several nonmutually exclusive mechanisms, including: (i) recruiting the positive transcription elongation factor complex (pTEFb) that is essential for RNA polymerase II–dependent transcription elongation (6, 7); (ii) activating pTEFb by directly phosphorylating CDK9 or its associated factors via an atypical kinase activity recently identified in BRD4 (8); (iii) serving as histone chaperones to structurally alter or remove the nucleosomal barrier to allow passage of elongating RNA polymerase II (9), and (iv) assembling active transcription complexes containing important transcription factors such as E2F-1 (10). Furthermore, it has been shown that BRD4 is highly enriched in super-enhancers that drive the expression of factors that are critical for the pathogenesis of cancer, suggesting that targeting BET family proteins could be a promising approach for cancer treatment (11). Using small-molecule inhibitors, such as JQ-1 and iBET, the potential benefit of targeting BET family proteins has been demonstrated in preclinical models of NUT midline carcinoma (NMC), acute myeloid leukemia (AML), multiple myeloma, acute lymphoblastic leukemia (ALL), non-Hodgkin lymphoma (NHL), non–small cell lung carcinoma (NSCLC), glioblastoma, neuroblastoma (NB), prostate cancer, and breast cancer (12–24). Objective clinical responses have been reported from phase I clinical trials in NMC, AML, NHL, and multiple myeloma using the BET inhibitor OTX015 (25–27). Here, we describe the comprehensive *in vitro* and *in vivo* characterization of a novel BET family bromodomain inhibitor, ABBV-075 (28). Results from this study revealed divergent BET inhibitor responses between solid tumors and hematologic malignancies, and uncovered potential cancer indication selection and combination strategies to guide the clinical development of ABBV-075 or other BET inhibitors.

Materials and Methods

Cells and antibodies

MV4:11, THP1, RS4:11, Kasumi, RPMI8226, SuDHL2, Raji, Ramos, Toledo, Pfeiffer, HT, RL, Farage, SuDHL4, DB, H1299, CAMA1, HCC1143, HCC1569, HCC1937, HCC38, Hs578T,

Oncology Discovery, AbbVie Inc., North Chicago, Illinois.

Note: Supplementary data for this article are available at Cancer Research Online (http://cancerres.aacrjournals.org/).

Corresponding Author: Yu Shen, AbbVie Inc., 1 North Waukegan Road, North Chicago, IL 60064. Phone: 847-936-1128; E-mail: yu.shen@abbvie.com

doi: 10.1158/0008-5472.CAN-16-1793

UACC812, A431, DLD1, NCI-H929, H838, BxPC3, HPAC were obtained from ATCC from 2005 to 2014. SKM1, ML2, MOLM13, AML2, AML5, OPM2, L363, DoHH2, SuDHL8, OCI-LY1, OCI-LY3, ULA, NUDUL1, WSU-NHL, NUDHL1, OCI-LY19, WSU-DLCL2, OCI-LY7, U2973, SuDHL5, SuDHL16, OCI-LY18, Ri1, KMS11 were obtained from DSMZ from 2005 to 2015. KMS11 and MX1 were obtained from JCRB and NCI, respectively, in 2014 to 2015. All cell lines were tested for mycoplasma using MycoAlert Detection Kit (Lonza), authenticated using GenePrint 10 STR Authentication Kit (Promega) in the period from 2013 to 2016, and grown in media recommended by the manufacturer. All antibodies were purchased from commercial sources as follows: antibodies against BCL-2 were from BD Biosciences; antibodies against BCL-XL, PUMA, and BIM were from Abcam; antibodies against CASPASE-3, -9, PARP, and c-MYC were from Cell Signaling Technology; antibodies against MCL-1 were from Santa Cruz Biotechnology; antibodies against β-actin were from Sigma.

Engineered cell lines

SKM1 and AML2 cells were transfected with pLOC or pLOC-*BCL-XL* (Thermo Scientific Open Biosystems) using the Neon electroporator (Invitrogen). Cells were selected with blasticidin. Similarly, SuDHL8 cells were electroporated with pLOC or pLOC-*BCL-2*. Western blot analysis was utilized to confirm the expression of these proteins in the cells.

TR-FRET binding assays

Alexa647-labeled MS417 was used as the fluorescent probe in assay buffer (20 mmol/L sodium phosphate, pH 6.0, 50 mmol/L NaCl, 1 mmol/L ethylenediaminetetraacetic acid disodium salt dihydrate, 0.01% Triton X-100, 1 mmol/L DL-dithiothreitol) containing His-tagged bromodomain, europium-conjugated anti-His antibody (Invitrogen PV5596) and Alexa Fluor 647-conjugated probe. After a 1-hour equilibration at room temperature, TR-FRET ratios were determined using an Envision multilabel plate reader.

Gene expression analysis using the QuantiGene Plex assay

Cells were plated onto 96-well plates in a volume of 100-μL media containing 10% FBS and incubated at 37 °C in an atmosphere of 5% CO_2 overnight before starting compound treatment. Cells were then harvested to carry out the branched DNA assay (bDNA) using the QuantiGene Plex Assay Kit (Affymetrix/Panomics) according to manufacturer's instruction. Processed samples were analyzed using the FLEXMAP3D instrument (Luminex). mRNA of genes of interest was normalized to β-2-microglobulin (B2M) and presented as fold change relative to vehicle control.

Cell viability assays

Cells were plated onto 96- or 384-well plates in their respective culture medium and incubated at 37°C in an atmosphere of 5% CO_2. After overnight incubation, a serial dilution of ABBV-075 was prepared and added to the plate. The cells were further incubated for 3 or 5 days, and the CellTiter-Glo assay (Promega) was then performed according to manufacturer's instruction to determine cell proliferation. Luminescence signal from each well was acquired using the Victor plate reader (PerkinElmer), and the data were analyzed using the GraphPad Prism software (GraphPad Software Inc.).

FACS analysis for cell cycle and apoptosis

Cells in log phase growth were treated with compounds for the designated time. Cells were harvested and processed according to manufacturer's protocols. For cell-cycle analysis, propidium iodide (PI)/RNase staining buffer from BD Pharmingen was used. For apoptosis analysis, PE Annexin V Apoptosis Detection Kit I from BD Pharmingen was used, by which Annexin V–positive cells were considered as apoptotic. All FACS analysis was performed on FACSCalibur.

Chromatin immunoprecipitation–qPCR

SKM-1 and H1299 cells were treated as described, then fixed with 1% formaldehyde for 7 or 10 minutes, respectively, at room temperature (RT) with direct addition of 1% formaldehyde (Thermo Scientific). The fixation was stopped with 1.25 mmol/L glycine for 5 minutes, followed by wash and collection in cold PBS and subsequent lysis [1% SDS, 10 μmol/L EDTA, 50 μmol/L Tris-Cl pH 8.0, 5 mmol/L sodium butyrate (Sigma), protease inhibitor cocktail tables (Roche)]. Chromatin was sheared using the Bioruptor (Diagenode), then diluted 1:4 with dilution buffer (0.01% SDS, 1.1% Triton X-100), 1.2 μmol/L EDTA, 16.7 μmol/L Tris-Cl pH 8.0, 167 μmol/L NaCl, 5 mmol/L sodium butyrate, protease inhibitor cocktail tablet. IP was performed by the IP-Star (Diagenode) with anti-BRD4 antibodies (Bethyl) or normal rabbit IgG (CST) and Protein G Dynabeads (LifeTech). Chromatin immunoprecipitations (ChIP) were washed once with TE and three times with wash buffer (100 mmol/L Tris-Cl pH 8.0, 500 mmol/L LiCl, 15 Igepal, 1% deoxycholic acid). Beads were resuspended in elution buffer (20 mmol/L $NaHCO_3$, 1% SDS, 150 mmol/L NaCl) and cross-links were reversed overnight at 65°C, followed by RNase A and proteinase K digestion at 45 °C for 1 hour. DNA was purified using ChIP DNA Clean & Concentrator (Zymo). qPCR was performed with SYBR (Perfecta, Quanta), using specific primers for *MYC* promoter [EpiTect, NM:_002467.3 (-)01 Kb], reported E1, E2, E3, E5 enhancer (29), *BCL2L1* (forward: 5′-tgaggacattgaagcacagag; reverse: 5'-atcagcctatttcatccgtcc), or *BCL2L1* super enhancer regions [Epitect, NM_001191.2 (+02Kb) and (+) 03Kb] and analyzed using $\Delta\Delta C_t$ method with negative control region.

Animal studies

All animal studies were conducted in a specific pathogen-free environment in accordance with the Internal Institutional Animal Care and Use Committee, accredited by the American Association of Laboratory Animal Care under conditions that meet or exceed the standards set by the United States Department of Agriculture Animal Welfare Act, Public Health Service policy on humane care and use of animals, and the NIH guide on laboratory animal welfare. Overt signs of dehydration, lack of grooming, lethargy, >15% weight loss and tumor volume >20% of body weight were used to determine tumor endpoint. For tumor models, a 1:1 mixture of 5×10^6 cells/Matrigel (BD Biosciences) per site or 1:10 tumor brie [MX-1; in S-MEM (MEM, Suspension, no calcium, no glutamine); Life Technologies Corporation] was inoculated subcutaneously into the right hind flank of female SCID-beige or female Fox Chase SCID (Charles River Labs) mice, respectively, on study day 0. Administration of compound was initiated at the time of size match. The tumors were measured by a pair of calipers twice a week starting at the time of size match and tumor volumes were calculated according to the formula $V = L \times W^2/2$ [V, volume (mm^3); L, length (mm); W, width (mm)].

Tumor growth inhibition, %TGI = 100 − mean tumor volume of treatment group/mean tumor volume of control group × 100.

Determination of drug–drug interactions

Synergistic activities of ABBV-075 and venetoclax or other chemotherapeutic agents were determined using the Bliss additivism model. In this model, the combined response C of both agents with individual effects A and B is C = A + B – (A▪B), where A and B represent the percentage of inhibition between 0 and 100. Response scores greater than 10 were considered synergistic.

Results

ABBV-075 is a potent and selective BET family bromodomain protein inhibitor

ABBV-075 is a novel inhibitor of BET family bromodomain proteins that recently entered phase I clinical trials (Fig. 1A; ClinicalTrials.gov identifier: NTC02391480; ref. 28). ABBV-075 bound to protein constructs containing both bromodomains of BRD2, BRD4, or BRDT with similar affinities (K_i = 1–2.2 nmol/L), but exhibits roughly 10-fold weaker potency toward the tandem bromodomain construct of BRD3 (K_i = 12.2 nmol/L; Fig. 1A). ABBV-075 had moderate activity towards EP300 (K_d = 87 nmol/L; 54-fold selectivity vs. BRD4), and potential weak activity toward SMARCA4 (63% inhibition at 1 μmol/L), but exhibits K_d > 1 μmol/L (>600-fold selectivity vs. BRD4) for the other 18 bromodomain proteins examined (Fig. 1B). Similar to what has been reported for other BET family inhibitors, on-target cellular activity of ABBV-075 was confirmed through downregulation of *MYC* in a variety of cancer cell lines at both the mRNA and protein levels. For example, ABBV-075 inhibited *MYC* transcription in SKM-1 cells with an IC_{50} of 1 nmol/L. The ability of ABBV-075 to inhibit *MYC* transcription may be partly attributed to its ability to BRD4 displacement from *MYC* regulatory regions, including the promoter and reported lineage-specific enhancer/super enhancer (Fig. 1C; Supplementary Fig. S1; ref. 29).

ABBV-075 has broad antiproliferative activities across cancer cell lines

Promising *in vitro* and *in vivo* activities of JQ-1 or iBET have been reported in a variety of cancer cell models (12–24). However, most of these studies focus on a particular cancer indication

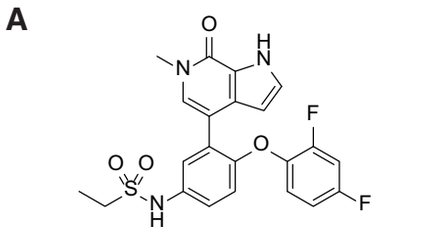

Compound	Tandem domain Ki (nmol/L)			
	BRD2	BRD3	BRD4	BRDT
ABBV-075	1	12.2	1.6	2.2

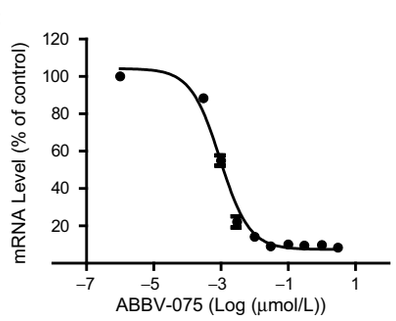

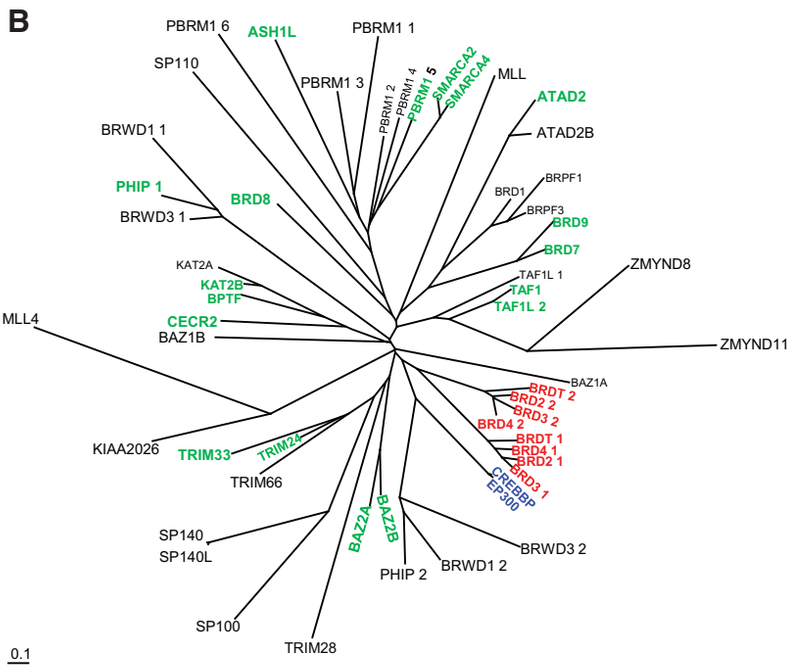

Figure 1.
ABBV-075 is a potent and selective BET family bromodomain inhibitor. **A,** Chemical structure of ABBV-075 and biochemical potencies determined by the TR-FRET assay. **B,** Selectivity of ABBV-075 across the phylogenetic tree of bromodomain containing proteins was determined using the BromoScan platform at DiscoveRx. Colors indicate proteins that were tested for ABBV-075 activity. Red, the branch for the BET family. ABBV-075 exhibits >600× selectivity against proteins (green), >50× selectivity against proteins colored in blue. **C,** SKM1 cells incubated with a series dilution of ABBV-075 for 6 hours, and *c-MYC* mRNA levels were determined by QuantiGene Plex assay and normalized to β-2-microglobulin (B2M) in each sample. The normalized expression level was used to determine the IC_{50} of ABBV-075. The concentration resulting in 50% inhibition of *c-MYC* expression (IC_{50}) was calculated using nonlinear regression analysis of the concentration response data. Results are representative of two independent experiments with biological duplicates in each experiment. Using hypoxanthine phosphoribosyltransferase (HPRT) or the geometric mean of HPRT and B2M instead of B2M as normalizers yielded similar results.

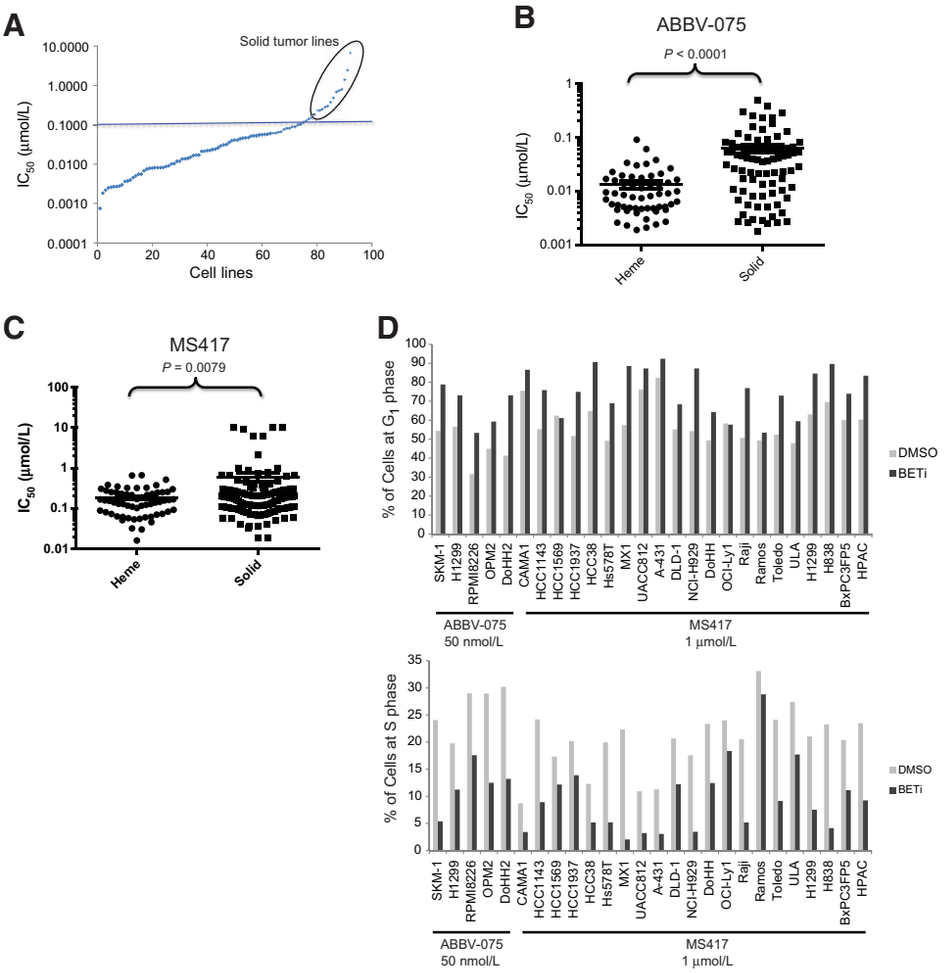

Figure 2.
ABBV-075 exhibited broad antiproliferative activities across cancer cell lines. **A,** IC_{50}s of ABBV-075 across cancer cell lines. IC_{50} is defined as the concentration at 50% of maximal possible response (50% growth inhibition). **B,** Comparison of ABBV-075 IC_{50} from the 5-day proliferation assay in cancer cell lines originated from hematologic malignancies versus solid tumors. **C,** Comparison of MS417 IC_{50} from the 5-day proliferation assay in cancer cell lines originated from hematologic malignancies versus solid tumors. **D,** Impact of MS417 and ABBV-075 on cell-cycle across cancer cell lines. Cell-cycle profiles were determined by FACS analysis using PI staining. Percentage of cells at G_1- and S-phase in cells exposed to DMSO or BET inhibitors at the indicated concentrations are presented.

without comparing sensitivities to BET inhibitors across different cancer indications. To identify sensitive cancer indications for ABBV-075 clinical development, we determined the antiproliferative activity of ABBV-075 using a 5-day proliferation assay across a panel of cancer cell lines representing multiple cancer indications. Under our assay conditions, ABBV-075 exhibited broad antiproliferative activities across 147 cancer cell lines with an IC_{50} of less than 0.1 μmol/L in more than 85% of these cell lines (Fig. 2A; Supplementary Table S1). All of the 21 ABBV-075–resistant cell lines ($IC_{50} > 0.1$ μmol/L) originated from solid tumors. Among the 126 cell lines that were sensitive to ABBV-075 ($IC_{50} < 0.1$ μmol/L), the hematologic cancer cell lines ($n = 56$) had a mean IC_{50} of 0.013 μmol/L versus a mean IC_{50} of 0.031 μmol/L in cell lines derived from solid tumors ($n = 70$), suggesting that cells originating from hematologic malignancies are somewhat more sensitive to ABBV-075 (Fig. 2B). Because some earlier studies using JQ1 and iBET indicated that BET inhibitors are highly active in cell lines from hematologic malignancies, but are largely inactive against most solid tumor cell lines examined, we further determined the activity of MS417 (30), a JQ1-like BET inhibitor that is about 10-fold less potent than ABBV-075 in TR-FRET assays, across a panel of more than 100 cancer cell lines. Similar to ABBV-075, MS417 was also broadly active and had slightly better sensitivities towards hematologic versus solid tumor cell lines, indicating that broad antiproliferative activity and moderate preference for hematologic malignancies may be characteristic of BET inhibitors in general (Fig. 2C; Supplementary Table S2). Consistent with the reported role of BRD4 in postmitotic transcription of genes required for cell-cycle progression, exposure to MS417 or ABBV-075 for 24 hours induced a clear increase in the G_1 population and a concurrent decrease in the S-phase population across solid and hematologic cancer cell lines examined, suggesting that G_1 cell-cycle arrest may be an important mechanism underlying the broad antiproliferative activity of BET inhibitors (Fig. 2D).

ABBV-075 triggers strong apoptosis in cell lines derived from hematologic malignancies

While most, if not all, sensitive cancer cell lines were arrested at G_1 when incubated with ABBV-075 for 24 hours, longer durations of treatment often led to a clear increase of sub-G_1 population in cells derived from hematologic malignancies, but not in cells derived from solid tumors, suggesting that there might be differences in apoptotic responses between cell lines of diverse origins. When 132 cell lines representing 20 cancer indications/subindications were examined for apoptosis in response to ABBV-075, strong apoptosis was observed in AML, NHL, and multiple myeloma cell lines, but not in many solid tumor-derived cell

lines except for N-myc–amplified neuroblastoma cells (Fig. 3A; Supplementary Table S3). Similar to what was observed with ABBV-075, MS417 also triggered high degrees of apoptosis in AML, NHL, and multiple myeloma cells, but not in cells originating from most solid tumors except for neuroblastoma (Supplementary Fig. S2 and Supplementary Table S4). Therefore, the selective induction of apoptosis in hematologic versus solid tumor cell lines may represent a class effect of BET inhibitors. In cell lines that exhibited strong apoptotic response to MS417, caspase cleavage became apparent within 24 hours of treatment (Fig. 3B). Time course studies using ABBV-075 in AML, multiple myeloma, and NHL cell lines further demonstrated that early apoptotic events such as caspase-3 activation and PARP cleavage can be detected at 8 to 16 hours post compound treatment (Fig. 3C).

ABBV-075 induces apoptosis in primary patient-derived cancer cells

To determine whether the noted apoptotic response to ABBV-075 can be recapitulated in primary patient-derived samples, we focused on AML, where patient-derived cells are readily available. Similar to what was observed in AML cell lines, patient-derived AML cells were also highly sensitive to ABBV-075 (IC_{50} < 0.1 μmol/L), and eight out of nine patient samples exhibited >30% apoptosis (Fig. 3D). It is noteworthy that many patient-derived AML cells appeared to be resistant to cytarabine, a first-line therapy for AML (e.g., pts 3027, 3235, 3012, and 3085, all with IC_{50}s ≥ 3 μmol/L), but remained responsive to ABBV-075, suggesting that ABBV-075 may provide benefit in the resistant/refractory setting of AML. As controls, no high degrees of apoptosis was observed in PBMCs from healthy donors, and ABBV-075 or MS417 did not trigger apoptosis in $CD34^+$ cells from cord blood (Supplementary Fig. S3).

BET inhibitor triggers apoptosis in AML/NHL/multiple myeloma cells by modulating the intrinsic apoptotic pathway

To obtain more insight on how BET inhibitors trigger apoptosis in hematologic malignancies, we examined the impact of BET inhibitors on the intrinsic apoptotic pathway. MS417 downregulated BCL-XL at 24 hours in nine out of the 10 AML and multiple myeloma cell lines that exhibited high degrees of apoptosis upon BET inhibitor treatment (Fig. 4A). Downregulation of BCL-2 and upregulation of BIM were also observed in some cell lines, but not as consistently as the reduction of BCL-XL. Interestingly, although MS417 did not downregulate BCL-XL or BCL-2 in the L363 cell line, there was a prominent increase of BIM and PUMA in these cells, suggesting that upregulation of proapoptotic proteins could be an alternative mechanism for BET inhibitors to induce apoptosis in specific cellular contexts. Although a decrease of MCL-1 occurred after 48 to 72 hours of compound treatment in many cell lines, examination of the responses of BCL-2 family proteins at earlier time points in SKM-1 cells indicated that the reduction of BCL-XL and BCL-2, but not MCL-1, was detectable at 16 hours, a time point at which early apoptotic events such as caspase activation and PARP cleavage were already apparent (Supplementary Fig. S4; Fig. 2D). These results suggest that MCL-1 downregulation is unlikely to be the primary cause of the apoptotic response triggered by BET inhibitors. Similar to what was observed with MS417, ABBV-075 also downregulated both BCL-XL and BCL-2 in SKM-1 cells and downregulated BCL-XL in AML-2 and OCI-Ly3 cells (Supplementary Fig. S5), indicating that modulating the intrinsic apoptotic machinery may be a common mechanism underlying apoptosis induced by BET inhibitors.

To further verify the involvement of BCL-XL in ABBV-075–induced apoptosis, we created SKM-1 and AML-2 cell lines that express an exogenous BCL-XL from the CMV promoter (the SKM1/Bcl-XL and AML2/Bcl-XL cells). Unlike endogenous BCL-XL in the parental or vector-integrated cells (SKM1 parental/SKM1 vector and AML2 parental/AML2 vector), BCL-XL expression from the CMV-promoter was increased rather than downregulated by ABBV-075 in the SKM1/Bcl-XL and AML2/Bcl-XL cells (Fig. 4B; Supplementary Fig. S6A). Although PARP cleavage was apparent in both the parental and vector-integrated cells treated with ABBV-075, PARP cleavage was undetectable in the SKM1/Bcl-XL cells and marginal in the AML2/Bcl-XL cells (Fig. 4B; Supplementary Fig. S6A). Annexin/7-AAD staining confirmed that the SKM1/Bcl-XL and AML2/Bcl-XL cells had much subdued, but not completely abolished apoptotic responses compared to the parental or vector-integrated cells, suggesting that ABBV-075–dependent modulation of the intrinsic apoptotic pathway is at least partially responsible for ABBV-075–induced apoptosis (Fig. 4C; Supplementary Fig. S6B). Notably, the SKM-1/Bcl-XL and AML2/Bcl-XL cells exhibited prominent G_1 arrest after exposure to 50 or 100 nmol/L ABBV-075 for 3 days. In contrast, the parental and vector-integrated SKM-1 and AML-2 cells exhibited strong apoptosis (as indicated by a clear increase of sub-G_1 population) rather than G_1 arrest under the same experimental conditions (Fig. 4D; Supplementary Fig. S6C). These data suggest that the induction of apoptosis and G_1 arrest are likely two independent activities of ABBV-075 that occur in parallel. The subdued apoptotic responses in the SKM1/Bcl-XL and AML2/Bcl-XL cells allow for the manifestation of the G_1 arrest phenotype that is otherwise masked by high degrees of apoptosis.

BCL-2 expression level and/or sensitivity to the BCL-2 inhibitor venetoclax potentially predict apoptotic responses to ABBV-075 in GCB-DLBCL cell lines

Compared with AML and multiple myeloma, where the majority of the cell lines [8/8 AML cell lines (100%) and 10/12 multiple myeloma cell lines (83%)] exhibited >30% apoptosis upon ABBV-075 treatment, the fraction of NHL cell lines that exhibited strong apoptosis is comparatively less [16/33 NHL cell lines (48%)]. High and low levels of apoptosis were observed in cell lines from the ABC and GCB subtypes, indicating that the degree of apoptotic response to ABBV-075 does not segregate according to the ABC or GCB subtypes. Within the ABC-DLBCL subtype, all three of the cell lines with MYD88 mutations are highly apoptotic upon ABBV-075 treatment. In comparison, the IKKβ inhibitor (IKK-2 inhibitor VI, CAS No. 354811-10-2) triggered apoptosis in both MYD88 wt and mutant cells, but not in the IKKβ-mutant line (Fig. 5A). Interestingly, GCB-DLBCL cells that are resistant to the selective BCL-2 inhibitor venetoclax (IC_{50} > 1 μmol/L; ref. 31) were found to exhibit higher levels of apoptosis upon ABBV-075 treatment (Fig. 5B). Western blot analysis also revealed that ABBV-075 is more likely to trigger high degrees of apoptosis in GCB-DLBCL cells that express low levels of BCL-2 (Fig. 5C). Importantly, overexpression of BCL-2 in SuDHL-8, a GCB-DLBCL cell line that expresses a very low level of BCL-2 and exhibits strong apoptotic response to ABBV-075, diminished ABBV-075-induced apoptosis, indicating that BCL-2 overexpression may have a mechanistic connection to low apoptosis in GCB-DLBCL cells upon ABBV-075 treatment (Fig. 5D). Collectively, these results

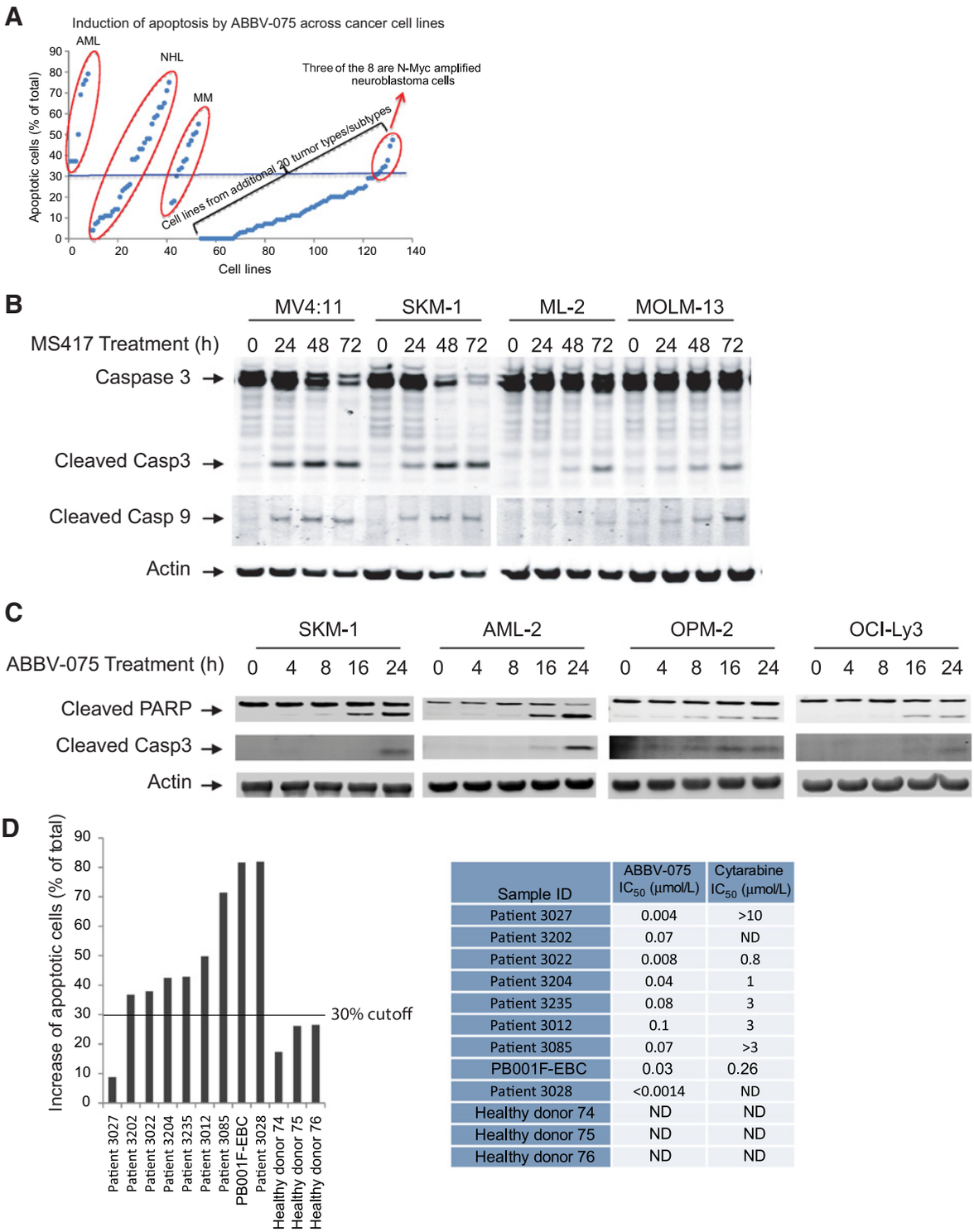

Sample ID	ABBV-075 IC_{50} (μmol/L)	Cytarabine IC_{50} (μmol/L)
Patient 3027	0.004	>10
Patient 3202	0.07	ND
Patient 3022	0.008	0.8
Patient 3204	0.04	1
Patient 3235	0.08	3
Patient 3012	0.1	3
Patient 3085	0.07	>3
PB001F-EBC	0.03	0.26
Patient 3028	<0.0014	ND
Healthy donor 74	ND	ND
Healthy donor 75	ND	ND
Healthy donor 76	ND	ND

Figure 3.

ABBV-075 induced higher degrees of apoptosis in cells originating from hematologic malignancies vs. solid tumors. **A,** Cells were treated with 0.2 μmol/L ABBV-075 for 72 hours and the degrees of apoptosis were determined by FACS analysis using Annexin and 7-AAD staining. Cells with positive Annexin or 7-AAD staining were scored as apoptotic cells. **B,** Cells were treated with 1 μmol/L MS417 for the indicated duration, lysed, and analyzed by Western blotting using antibodies against caspase-3, caspase-9, and actin. **C,** Cells were treated with 0.2 μmol/L ABBV-075 for the indicated duration, lysed, and analyzed by Western blotting using antibodies against PARP, caspase-3, and actin. Results in **B** and **C** are representative of two independent experiments. **D,** PBMCs from AML patients and healthy donors were tested for their responses to ABBV-075 and cytarabine. IC_{50}s were generated from dose responses to compounds in a 3-day proliferation assay with triplicates. Percentage of apoptosis was determined by incubating PBMC samples with 0.3 μmol/L ABBV-075 for 72 hours, followed by FACS analysis using Annexin/7-AAD staining. ND, not determined.

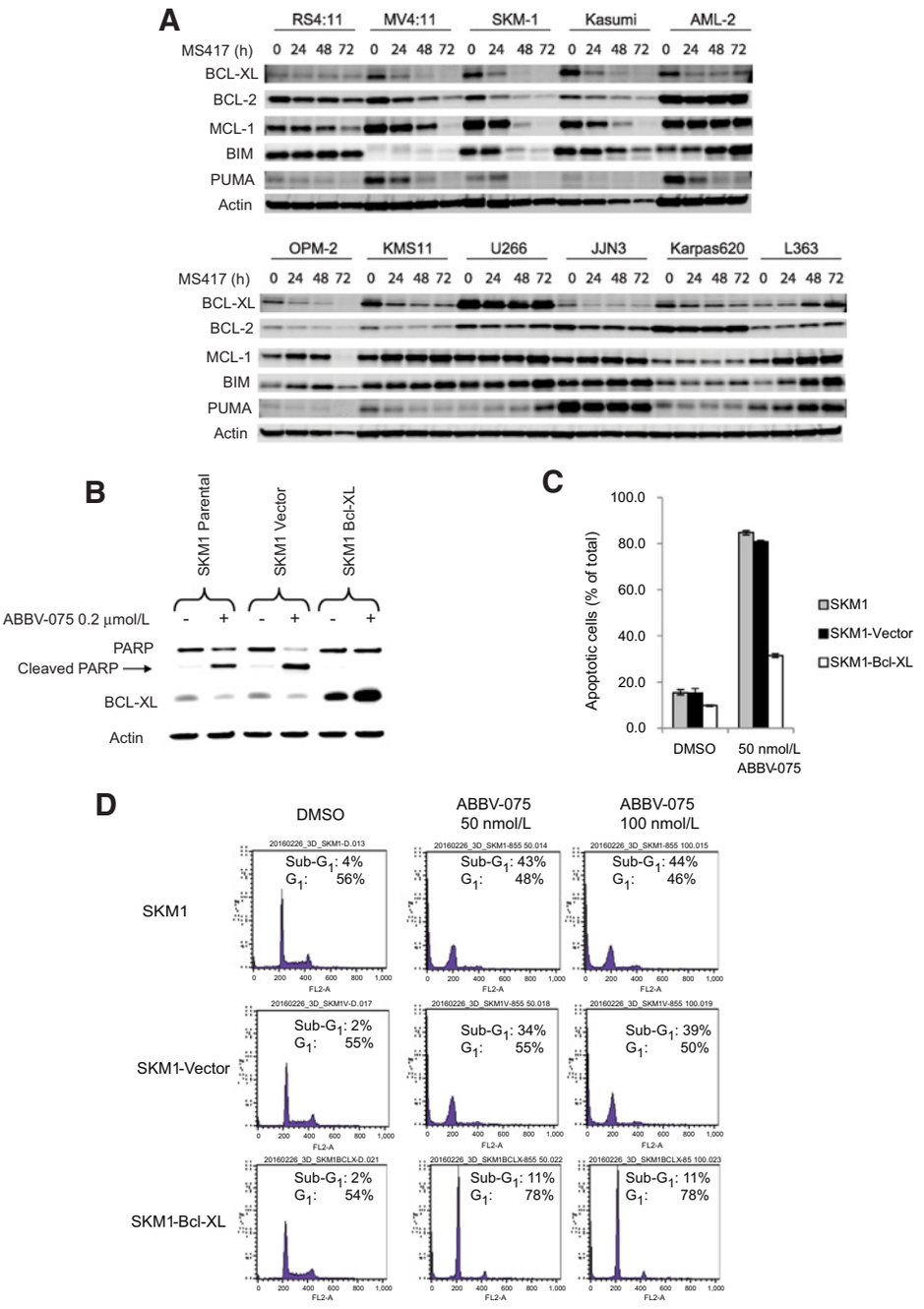

Figure 4.
BET family bromodomain inhibitors modulated the intrinsic apoptotic pathway. **A,** Cells were treated with 1 μmol/L MS417 for the indicated duration, collected at each time point, and analyzed by Western blotting using the indicated antibodies. **B,** SKM1 parental cells (SKM1 parental) and SKM1 cells with stable integrated empty vector (SKM1 vector) or Bcl-XL expression cassette (SKM1-Bcl-XL) were incubated without or with (− or +) 0.2 μmol/L ABBV-075 for 24 hours. Cells were then collected and analyzed by Western blotting. **C,** SKM1 parental cells (gray bars), cells with stably integrated empty vector (black bars), or Bcl-XL expression cassette (white bars) were incubated with DMSO or the indicated concentrations of ABBV-075 for 72 hours, then analyzed by FACS using Annexin/7-AAD staining to determine degrees of apoptosis. **D,** Cells were incubated with DMSO or indicated concentrations of ABBV-075 for 24 hours and cell-cycle profiles were analyzed by FACS using PI staining. All results are representative of two or more independent experiments.

suggest that BET inhibitors and venetoclax may have complementary activities in the GCB-DLBCL population, and the BCL-2 expression level or the prior response to venetoclax may be used to identify subpopulations of GCB-DLBCL that are more likely to exhibit apoptosis upon the treatment with BET inhibitors (31).

ABBV-075 exhibits synergy with venetoclax

Consistent with its antiproliferative and proapoptotic activity in hematologic cancer cell lines, ABBV-075 produced antitumor efficacies in xenograft tumor models representing AML, multiple myeloma, and NHL (Fig. 6A and B). In these models, the degree of tumor growth inhibition (TGI) achieved from ABBV-075 treatment is often equivalent to or greater than that achieved from treatment with the relevant standard of care agents for the same indication. To explore the potential utility of ABBV-075 in combination with other oncology agents, we examined the *in vitro* activity in AML/multiple myeloma/NHL cells (three cell lines/indication) for the combinations of ABBV-075 or MS417 with commonly used cancer drugs and emerging therapeutics for these indications, which include azacitidine, cytarabine, daunarubicin, cyclophosphamide, vincristine, bortezomib, iMIDs, ibrutinib, HDAC inhibitor, Flt3 inhibitor, PI3Kδ/γ

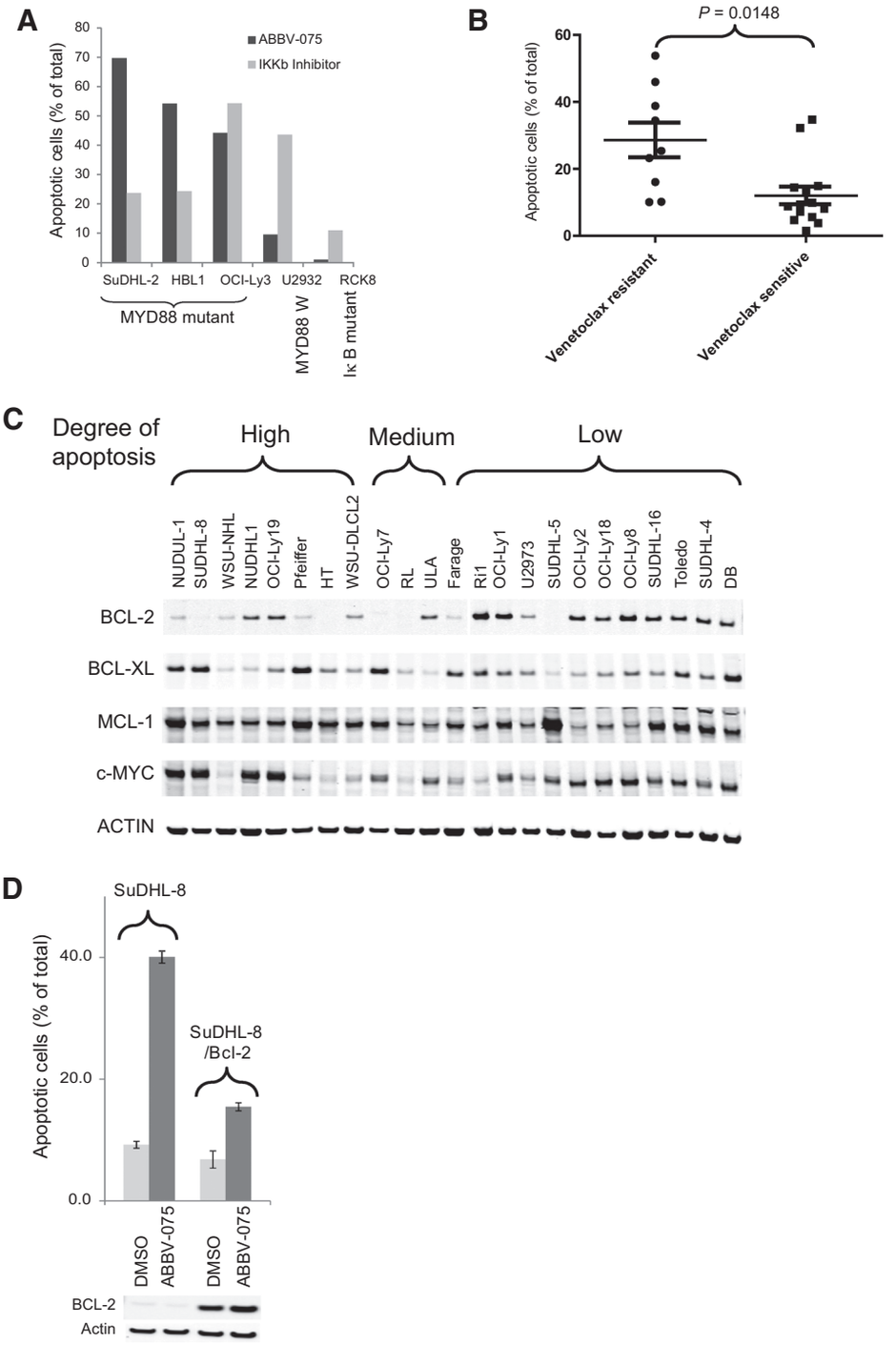

Figure 5.
Sensitivity to venetoclax or Bcl-2 expression level partly predicted the degree of apoptotic responses to ABBV-075 in GCB-DLBCL cells. **A,** Cells were incubated with 0.2 μmol/L ABBV-075 or 5 μmol/L of the IKK inhibitor (IKK-2 inhibitor VI, Calbiochem) for 72 hours and degrees of apoptosis were determined by FACS analysis using Annexin/7-AAD staining. **B,** Comparison of apoptotic responses to ABBV-075 in GCB-DLBCL cell lines that are sensitive (IC_{50} < 1 μmol/L) or resistant (IC_{50} > 1 μmol/L) to venetoclax. Sensitivity to venetoclax was based on the published results. **C,** Expression levels of BCL-2 family proteins and c-MYC in GCB-DLBCL cell lines that exhibited different degrees of apoptosis upon 72 hours of ABBV-075 treatment. High, >20% apoptotic cells; Medium, 10%-20% apoptotic cells; Low, <10% apoptotic cells. **D,** SuDHL-8 parental cells (SuDHL-8) and SuDHL-8 cells with an integrated exogenous BCL-2 expression cassette (SuDHL-8/Bcl-2) were incubated with DMSO or 0.1 μmol/L ABBV-075 for 72 hours, then analyzed by FACS using Annexin/7-AAD staining or Western blotting to determine levels of BCL-2 and actin. All results are representative of two or more independent experiments.

inhibitor, and venetoclax. Although most of these agents failed to exhibit strong synergy with BET inhibitors under our experimental conditions, ABBV-075 at 0.2 μmol/L caused a roughly 100-fold shift of the venetoclax dose–response curve in a 24-hour cell viability assay in AML-5 and THP-1 cells, and synergistic Bliss scores were observed in a broad dose range of both compounds (Fig. 7A). Further studies using ABBV-075 and/or MS417 demonstrated that BET inhibitors exhibited synergy with venetoclax across AML cell lines, including SKM-1, THP-1, AML5, MV4:11, ML-2, MOLM-13, AML-2, Kasumi, and HL-60. The *in vitro* synergy of ABBV-075 and venetoclax also translated to enhanced efficacy using the combination regimen versus monotherapies of each compound in the SKM1 model (Fig. 7B). Taken together, these results suggest that the combination of ABBV-075/venetoclax may warrant further investigation in AML.

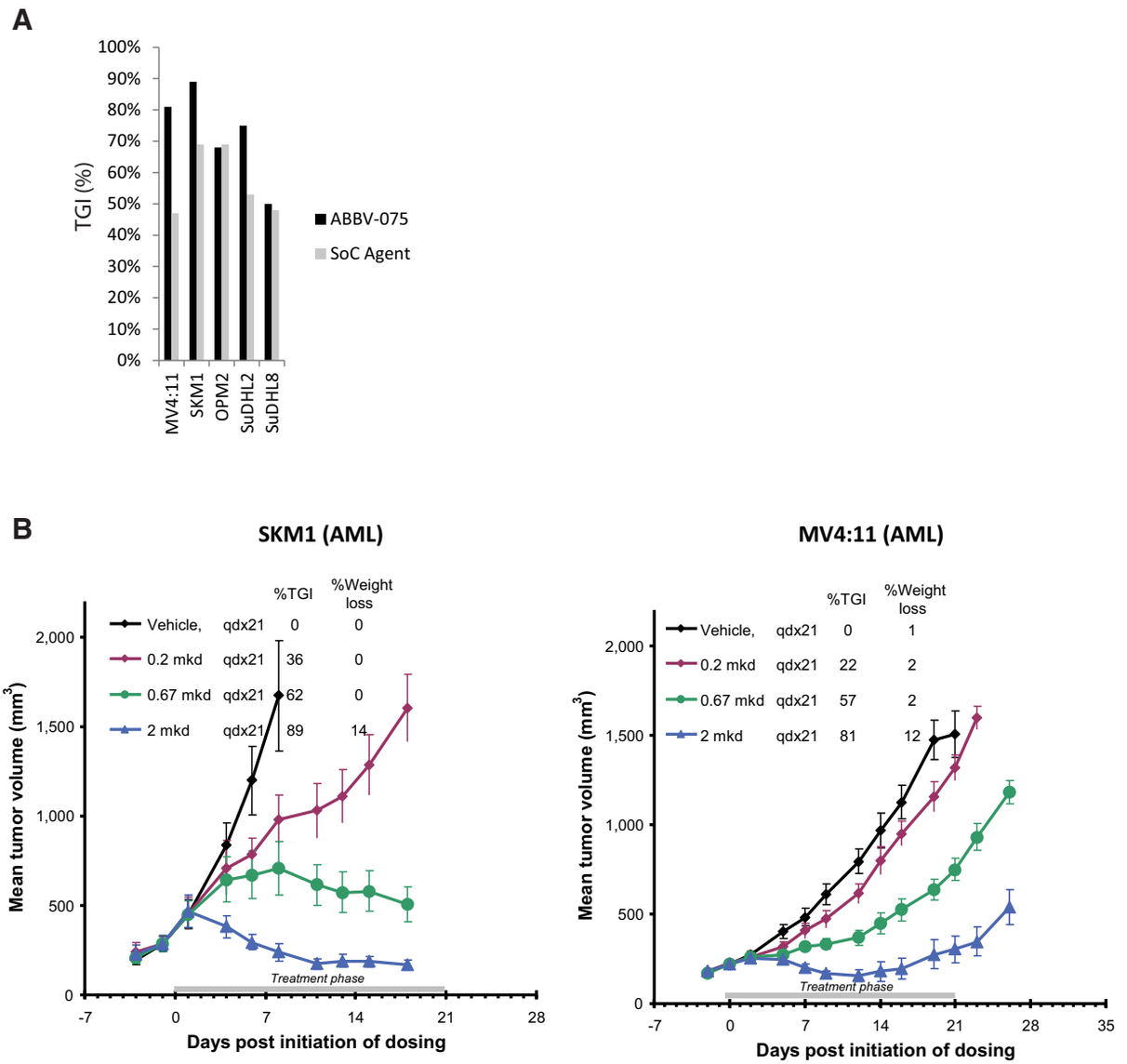

Figure 6.

ABBV-075 exhibited antitumor efficacy in xenograft models of hematologic malignancies. **A,** Summary of antitumor efficacy of ABBV-075 in xenograft tumor models of AML, multiple myeloma, and NHL. TGI was calculated using the formula: 100 × the size of treatment group/size of vehicle control group. TGI of ABBV-075 was calculated from the ABBV-075 dosing group of 1 mg/kg per day, orally, qd × 21. TGI of standard care agents are representative results based on historical data in the same model. **B,** *Scid*-Beige mice bearing the SKM1 tumor and *scid* mice bearing the MV4:11 tumors were dosed with vehicle or ABBV-075 at the indicated amounts and frequencies using oral gavage for 21 days (orally, qd × 21). qd, ABBV-075 was administered once every day. Tumor growth was monitored by tumor size measurement using a caliper, and the mean and SEM of tumor size for each treatment group are presented. TGI was calculated using the formula: 100× the size of treatment group/size of vehicle control group. %WL (%weight loss) represents the maximal percentage of weight loss in each dosing group during the entire course of the study. All results are representative of two or more independent experiments, with $n = 10$ per treatment group.

Low doses of ABBV-075 enhance the activity of azacitidine and bortezomib in xenograft models of AML and multiple myeloma, respectively, despite a lack of *in vitro* synergy

Although we did not observe *in vitro* synergy between ABBV-075 and azacitidine, cytarabine, or bortezomib in relevant cancer cell lines, to thoroughly probe the potential impact of incorporating ABBV-075 into the standard of care regimen in AML and multiple myeloma, we directly tested the combinations of ABBV-075 with azacitidine and bortezomib in xenograft models of AML (MV4:11, SKM1) and multiple myeloma (OPM2). To our surprise, despite the lack of *in vitro* synergy with azacitidine and bortezomib in the SKM1 and OPM2 cells, ABBV-075, at relatively low doses, enhanced the activities of azacitidine and bortezomib in SKM1 and OPM2 xenograft tumors, respectively. As shown in Figure 7C, ABBV-075 at 0.25 mg/kg/day, when combined with bortezomib, caused a deeper tumor response than bortezomib alone and a

longer delay of tumor progression after treatment withdrawal. Likewise, combining azacitidine with ABBV-075 at 0.67 mg/kg/day resulted in a tumor response that was superior to monotherapies of either agent alone (Fig. 7D). Therefore, using a low dose of ABBV-075 in combination with azacitidine, bortezomib, or venetoclax may represent attractive opportunities to derive antitumor benefit without triggering overt BET inhibitor–related toxicities.

Discussion

Targeting epigenetic readers such as the BET family bromodomain proteins has emerged as a promising approach for the development of cancer therapeutics, and a number of BET family bromodomain inhibitors are being investigated in clinical trials. The potential efficacy of BET inhibitors has been extensively explored in preclinical models of many cancer indications using tool compounds such as JQ1 and iBET. However, most of these studies focus on a particular cancer indication without cross comparing sensitivities of different cancer indications to BET inhibitors. Here we present an extensive *in vitro* and *in vivo* characterization of a novel BET inhibitor, ABBV-075, across preclinical models representing many cancer indications.

Our results demonstrated that BET inhibitors have broad antiproliferative activities across cancer cell lines and are highly active in tumor models representing hematologic malignancies. G_1 cell-cycle arrest appears to be a common response to BET inhibitors in cancer cells. However, after the initial response of cell-cycle arrest at 24 hours, cells originating from solid tumors and hematologic malignancies often follow different fates. Most cells originating from solid tumors can be arrested at G_1 for many days without extensive apoptosis. In these cells, cell-cycle arrest is reversible in the short term, and most cells can reenter the cell cycle within 24 hours of compound withdrawal (Supplementary Fig. S7). However, longer exposure to ABBV-075 or MS417 (e.g., 7 days or longer) can trigger senescence in many of these cell lines (Supplementary Fig. S8). The relatively universal G_1 arrest phenotype following BET inhibitor treatment is consistent with the reported role of BRD4 in post mitotic transcription of genes that are important for cell-cycle progression. In our hands, we also observed the downregulation of genes important for cell-cycle regulation in the H1299 and SKM1 cells after ABBV-075 treatment (Supplementary Fig. S9). In the literature, the ability of BET inhibitors to modulate disease specific pathogenic factors is often highlighted as the primary driver of their activity in various cancer settings (13, 15, 18, 21, 22, 24). A better understanding of the interplay and relative contribution of the general cell-cycle arrest mechanism versus disease- or pathway-specific mechanisms to the potential efficacy of BET inhibitors, particularly in solid tumor indications, could shed light on where and when to use BET inhibitors as cell-cycle blockers or pathway-specific targeted therapies.

Unlike the sustained G_1 arrest phenotype observed in cells derived from solid tumors, cell death often occurred at or after 24 hours of treatment with BET inhibitors in cells originating from hematologic malignancies. The degree of apoptosis induced by ABBV-075 appears to be higher compared with what was reported for OTX015 in a limited set of NHL cell lines (32). We suspect this is likely due to the better potency of ABBV-075 (>50× more potent in binding assays) or unknown differences of culturing and treatment conditions (33). Apoptosis induced by BET inhibitors is, at least in part, due to the modulation of the intrinsic apoptotic machinery. Downregulation of BCL-XL and, in some cellular context, downregulation of BCL-2 and/or upregulation of BIM/PUMA may contribute to the apoptotic response triggered by BET inhibitors. Downregulation of *BCL-XL* mRNA was observed after 4 hours of ABBV-075 treatment across cancer cell lines, with slightly stronger inhibition in cells that exhibited higher degrees of apoptosis (Supplementary Fig. S10). In SKM1 and H1299 cells, ABBV-075 displaced BRD4 from the *BCL-XL* promoter and a reported super enhancer (Supplementary Fig. S11; ref. 34). However, given the similar activities of ABBV-075 on these regulatory regions in the highly apoptotic SKM1 and less apoptotic H1299 cells, it remains to be determined whether there are unidentified Bcl-XL super-enhancers that may display different responses to ABBV-075 treatment to help explaining the stronger Bcl-XL downregulation in highly apoptotic cells.

We suspect that, beyond the slight differences on Bcl-XL downregulation, there will be additional factors contribute to differential sensitivity to ABBV-075 across cancer cell lines. We examined genomic alternations of important tumor suppressors/oncogenes and the expression of genes that reportedly influence sensitivity of BET inhibitors for their association with degrees of apoptosis induced by ABBV-075 (23, 35–38). No significant differences ($P < 0.05$) were observed in highly apoptotic (>30% apoptosis) versus low apoptotic (<30% apoptosis) cells for the expression, copy number alteration, or mutation of p53, PTEN, RB mutation, Myc amplification, the expression of CCAT1 (a gene associated with sensitivity to BETi in colon cancers), Trim33 (whose loss causes resistance to BETi), genes that reflect Wnt/β-catenin pathway activity (*TCF4*, *Axin*, *HOXB6*, *HOXC10*, *AXIN2*, *CCND1*, *IGF2BP1*, *TCF4*, *CCND2*, *HOXB4*, *FZD5*), or genes relevant to BRD4 phosphorylation (*CSNK2A1*, *CSNK2A2*, *CSNK2B*, *PPP2CA*, *PPP2CB*). In addition, genomic background in AML, such as MLL fusion, FLT3-ITD, NPM mutation, PTPN11 mutation, or chromatin translocations that lead to Myc overexpression in NHL or multiple myeloma are also not associated with apoptotic responses to ABBV-075. Although PPP2CB expression is significantly different in apoptotic versus nonapoptotic cells ($P < 0.05$), higher PPP2CB was observed in low apoptotic cells, which is at the opposite direction of the reported hypothesis (23). In addition, the PP2A activator PTZ did not sensitize cells such as H1299 or 22RV1 to ABBV-075–induced apoptosis, further indicating that CK2 activation or PP2A inactivation is unlikely to be critical contributors to the resistance to ABBV-075–induced apoptosis in our dataset (Supplementary Fig. S12).

cMyc expression (but not Myc amplification) is significantly higher in apoptotic cells ($P < 0.01$). However, introducing exogenously expressed cMyc that was not downregulated by MS417 into apoptotic cells (e.g., MV4:11 cells) failed to rescue these cells from apoptosis or growth arrest (Supplementary Fig. S13). Considering the strong trend of higher Myc expression in hematologic versus solid tumor histology across the entire CCLE cell line panel, these data collectively suggest that Myc expression may not be functionally linked to apoptotic response to BETi but rather segregated with the hematologic histology.

Importantly, high apoptotic cell lines exhibited higher levels of Bim, Bcl-2, and slightly lower levels of Bcl-XL compared to low apoptotic cell lines. In contrast, Mcl1 expression is not significantly different between the two populations. Consistent with the dominance of hematologic cancer cells among the apoptotic cell population, the same expression preferences of these genes were

A

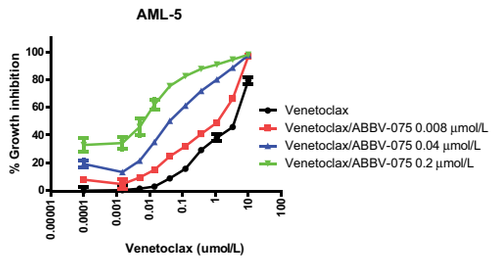

Bliss Excess Score					
			ABBV-075 (µmol/L)		
		DMSO	0.008	0.040	0.200
Venetoclax	0	0.0	0.2	0.2	0.2
	0.001	0.0	-3.3	-6.0	1.3
	0.004	0.0	0.4	1.3	12.2
	0.013	0.0	4.7	13.7	27.4
	0.04	0.0	8.9	24.1	36.8
	0.123	0.0	9.9	29.5	39.4
	0.37	0.0	6.1	29.2	35.4
	1.11	0.0	6.2	30.2	32.6
	3.33	0.0	16.3	32.4	31.0
	10	0.0	15.8	14.2	11.8

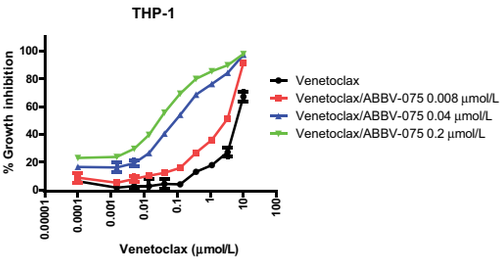

Bliss Excess Score					
			ABBV-075 (µmol/L)		
		DMSO	0.008	0.040	0.200
Venetoclax	0	0.0	-5.8	-5.3	-4.9
	0.001	0.0	-5.3	-1.8	-0.6
	0.004	0.0	-3.5	0.3	4.3
	0.013	0.0	-1.3	7.5	14.3
	0.04	0.0	-0.6	20.2	29.2
	0.123	0.0	3.3	33.9	42.9
	0.37	0.0	5.9	41.0	46.8
	1.11	0.0	10.8	44.6	48.5
	3.33	0.0	17.7	44.8	45.7
	10	0.0	21.3	24.6	23.0

B

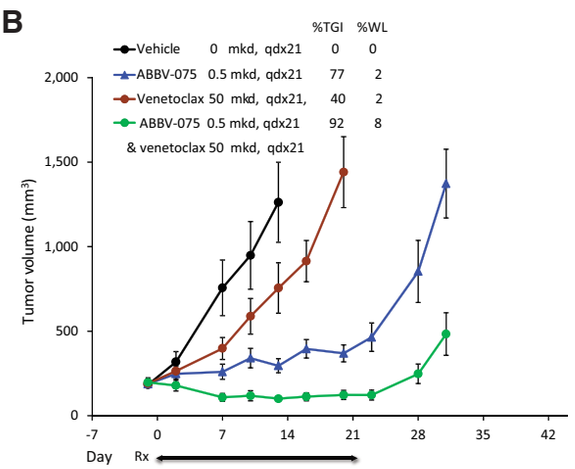

C

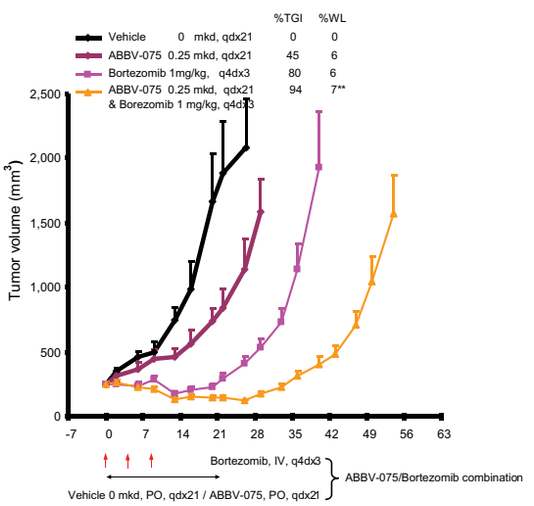

D

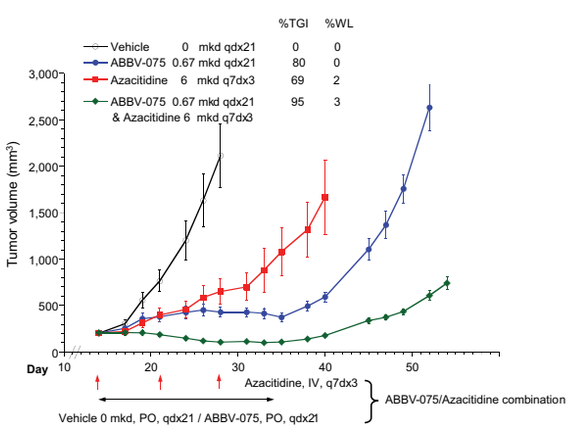

also observed in hematologic versus solid tumor cells (Supplementary Fig. S14). We hypothesized that high basal levels of Bim expression may exert strong apoptotic stress, and high Bcl-2 expression is an adaptive response to maintain an intricate balance between proapoptotic and antiapoptotic capacity. Under these conditions, downregulation of Bcl-XL by ABBV-075 is sufficient to tip the balance to trigger apoptosis. In contrast, many solid tumor cell lines lack the proapoptotic stress from high levels of Bim expression. Therefore, the antiapoptotic capacity exceeds the proapoptotic capacity in these cells. Consequently, moderate downregulation of Bcl-XL by ABBV-075 is not sufficient to tip the balance to trigger cell death (Supplementary Fig. S15). As a support for this model, the previously described Granta519 cells with low level of Bim expression were found to exhibit much less apoptosis in response to ABBV-075 compared to the parental cells (Supplementary Fig. S16), suggesting that high levels of Bim expression is required for strong apoptotic responses to ABBV-075.

Because Bim and Bcl2 expression are the two most significant factors (both with $P < 0.0001$) that separate high versus low apoptosis cells in our dataset, we searched the CCLE cell lines for cells that concomitantly express high levels of Bim and Bcl-2. This analysis revealed that relatively large percentages of AML, NHL, multiple myeloma, and NB cells meet the criteria, thus likely to exhibit apoptotic responses to ABBV-075 treatment, which is consistent with the experimental data described earlier (Supplementary Fig. S17). Interestingly, this analysis identified SCLC as a solid tumor indication that might exhibit apoptotic responses to ABBV-075 (Supplementary Fig. S17). Because of technical difficulties such as strong cell aggregation and high background apoptosis without compound treatment, SCLC cell lines were not included in the large panel of cell lines that were used to determine apoptotic responses to ABBV-075 in our study. However, an elegant independent study that determined responses of a panel of SCLC cell lines to ABBV-075 revealed that 9 out of 14 SCLC cell lines underwent strong apoptotic responses (>30% apoptotic cells) upon exposure to ABBV-075 (Lam et al. MCT, under revision), thus providing further support that high levels of both Bim and Bcl-2 expression may be predictive of apoptotic responses to ABBV-075.

Considering the generally better sensitivity of BET inhibitors against cell lines originating from hematologic malignancies and the strong apoptosis observed in AML, multiple myeloma, and subpopulations of NHL, these cancer types could be "low hanging fruits" for the development of BET inhibitors. The strong efficacy obtained by combining sub-MTD doses of ABBV-075 with venetoclax, azacitidine, or bortezomib indicates that these combinations may represent attractive opportunities to derive clinical benefit from BET inhibitors. There are many unanswered questions regarding these combinations. Despite diligent exploration of multiple experimental conditions, we failed to observe synergy between ABBV-075 and azacitidine *in vitro*. Microarrays analysis of tumors samples after single agent or combination treatment of ABBV-075 and azacitidine revealed that a single dose of azacitidine enhanced the transcriptional modulation of a small subset of ABBV-075-responsive genes 3 days later. Genes whose regulation by ABBV-075 was enhanced by azacitidine included Bcl-2, Myb, SCD, CDKN1A, and many genes related to inflammatory responses (Supplementary Fig. S18). Extensive follow-up studies will be required to establish whether and/or how these transcriptional alterations contribute to the antitumor efficacy of the ABBV-075/azacitidine combination.

Similarly, we also did not detect synergy between ABBV-075 and bortezomib in tissue culture. In addition, potential tumor environmental factors such hypoxia and prosurvival cytokines such as IL6 did not obviously alter cancer cell responses to ABBV-075. Therefore, it is unlikely that bortezomib treatment reverses resistance to ABBV-075 in tumor microenvironment and consequently results in strong antitumor efficacy with the combination regimen (Supplementary Fig. S19). However, consistent with the recently reported anti-angiogenesis activity of BET inhibitors (39), exposure of ABBV-075 inhibited HUVEC cell proliferation and blocked the expression of angiogenesis factors such as VEGF and PDGF under hypoxia, suggesting a potential anti-angiogenesis role of ABBV-075 (Supplementary Fig. S20). It is noteworthy that iMIDs such as lenalidomide possess anti-angiogenesis activities and exhibit strong antitumor efficacy in combination with bortezomib in multiple myeloma. We suspect that the strong efficacy obtained using ABBV-075/bortezomib combination maybe partly attributed to the impact of ABBV-075 on tumor angiogenesis.

Although AML/multiple myeloma/NHL may represent relatively "low hurdle" choices for BET inhibitors, the broad antiproliferative activities of BET inhibitors against solid tumor cell lines suggest potential opportunities for using BET inhibitors in solid tumors. In some solid tumor cell lines, both ABBV-075 and MS417 have IC_{50}s in the same range as some of the most sensitive hematologic cancer cells. Defining biomarkers that allow the enrichment of these highly sensitive tumors could greatly improve the probability of success for BET inhibitors in solid tumor settings. In addition, it is worthwhile to note that beyond their abilities to inhibit cancer cell proliferation or survival, BET inhibitors could exert a multifaceted impact on tumor microenvironment or other aspects of tumor biology. For example, *c-MYC*, one

Figure 7.

Sub-MTD doses of ABBV-075 enhanced the activities of venetoclax, azacitidine, and bortezomib in xenograft models of AML and multiple myeloma. **A,** Left, dose–response curve of venetoclax in the absence or presence of indicated amounts of ABBV-075 in AML5 and THP1 cells. Right, Bliss excess score calculated based on the dose-responses presented in the left panel. A Bliss excess score >10 indicates strong synergy and was colored gray. **B,** Mice bearing SKM1 tumors were administered with vehicle, monotherapies of venetoclax or ABBV-075, or the combination of ABBV-75/venetoclax at the indicated dose and schedule. **C,** Mice bearing the OPM2 tumors were administered with vehicle, monotherapies of bortezomib or ABBV-075 at the indicated dose and schedule, or the combination of bortezomib with ABBV-075. Red arrow, administration of bortezomib. *, two mice were removed from study due to weight loss. **D,** Mice bearing the SKM1 tumors were administered with vehicle, monotherapies of azacitidine or ABBV-075 at the indicated dose and schedule or the combination of azacitidine with ABBV-075. Red arrow, administration of azacitidine. In **B**, **C**, and **D**, tumor growth was monitored by tumor size measurement using a caliper, and the mean and SEM of tumor size for each treatment group are presented. TGI was calculated using the formula: 100 × the size of treatment group/size of vehicle control group. %WL (%weight loss) represents the maximal percentage of weight loss in each dosing group during the entire course of the study. All results are representative of two or more independent experiments, with duplicates in each experiments for *in vitro* proliferation assay and $n = 10$ per treatment group for *in vivo* efficacy studies.

of the best-defined targets of BET inhibitors, has been shown to be critical for the maintenance of the tumor microenvironment that supports pancreatic tumors in genetically engineered mouse tumor models (40). We also observed that exposure to BET inhibitors such as ABBV-075 and MS417 caused strong inhibition of HUVEC cell proliferation and blocked the expression of angiogenesis factors such as VEGF and PDGF under hypoxia, suggesting a potential impact of BET inhibitors on tumor angiogenesis and/or hypoxia response. Furthermore, in AML cells that are relatively resistant to ABBV-075-induced apoptosis, ABBV-075 triggered the expression of differentiation markers CD11b and CD14, suggesting that ABBV-075 may produce antitumor efficacy by inducing growth arrest and differentiation in some cancer settings (Supplementary Fig. S21). Further exploration of the activity of BET inhibitors toward many different aspects of cancer biology may help identify additional cancer types that may benefit from BET inhibitors as a monotherapy or in combination.

Disclosure of Potential Conflicts of Interest

G.S. Sheppard has ownership interest (including patents) in AbbVie, Inc. S. Fidanze has ownership interest (including patents) in AbbVie. G. Fang has ownership interest (including patents) in AbbVie stock. K.F. McDaniel has ownership interest (including patents) in AbbVie. W.M. Katti has ownership interest (including patents) in stocks. No potential conflicts of interest were disclosed by the other authors.

Authors' Contributions

Conception and design: X. Lin, D.H. Albert, L. Li, L.T. Lam, S.E. Warder, S. Fidanze, J.K. Pratt, D. Liu, T. Uziel, F. Kohlhapp, G. Fang, S.H. Rosenberg, K.F. McDaniel, Y. Shen

Development of methodology: L. Li, E.J. Faivre, S.E. Warder, X. Huang, J.K. Pratt, D. Liu, F. Kohlhapp

Acquisition of data (provided animals, acquired and managed patients, provided facilities, etc.): M.H. Bui, D.H. Albert, L. Li, L.T. Lam, X. Huang, D. Wilcox, C.K. Donawho, G.S. Sheppard, S. Fidanze, T. Uziel

Analysis and interpretation of data (e.g., statistical analysis, biostatistics, computational analysis): M.H. Bui, X. Lin, D.H. Albert, L. Li, L.T. Lam, E.J. Faivre, X. Huang, T. Uziel, X. Lu, F. Kohlhapp, Y. Shen

Writing, review, and/or revision of the manuscript: X. Lin, D.H. Albert, L. Li, L.T. Lam, E.J. Faivre, S.E. Warder, X. Huang, C.K. Donawho, G.S. Sheppard, L. Wang, S. Fidanze, J.K. Pratt, D. Liu, L. Hasvold, F. Kohlhapp, S.W. Elmore, S.H. Rosenberg, K.F. McDaniel, W.M. Kati, Y. Shen

Administrative, technical, or material support (i.e., reporting or organizing data, constructing databases): M.H. Bui, L.T. Lam, X. Huang

Study supervision: X. Lin, D.H. Albert, L.T. Lam, G. Fang, S.W. Elmore, W.M. Kati, Y. Shen

Other (Participated in medicinal chemistry activities leading to the discovery of generation of ABBV-075 for characterization.): L. Wang, L. Hasvold, K.F. McDaniel

The costs of publication of this article were defrayed in part by the payment of page charges. This article must therefore be hereby marked *advertisement* in accordance with 18 U.S.C. Section 1734 solely to indicate this fact.

Received July 6, 2016; revised August 30, 2016; accepted April 6, 2017; published OnlineFirst April 17, 2017.

References

1. Arif M, Senapati P, Shandilya J, Kundu TK. Protein lysine acetylation in cellular function and its role in cancer manifestation. Biochim Biophys Acta 2010;1799:702–16.
2. Singh BN, Zhang G, Hwa YL, Li J, Dowdy SC, Jiang SW. Nonhistone protein acetylation as cancer therapy targets. Expert Rev Anticancer Ther 2010;10:935–54.
3. Mujtaba S, Zeng L, Zhou MM. Structure and acetyl-lysine recognition of the bromodomain. Oncogene 2007;26:5521–7.
4. Sanchez R, Zhou MM. The role of human bromodomains in chromatin biology and gene transcription. Curr Opin Drug Discov Dev 2009;12:659–65.
5. Gaucher J, Boussouar F, Montellier E, Curtet S, Buchou T, Bertrand S, et al. Bromodomain-dependent stage-specific male genome programming by Brdt. EMBO J 2012;31:3809–20.
6. Jang MK, Mochizuki K, Zhou M, Jeong HS, Brady JN, Ozato K. The bromodomain protein Brd4 is a positive regulatory component of P-TEFb and stimulates RNA polymerase II-dependent transcription. Mol Cell 2005;19:523–34.
7. Yang Z, Yik JH, Chen R, He N, Jang MK, Ozato K, et al. Recruitment of P-TEFb for stimulation of transcriptional elongation by the bromodomain protein Brd4. Mol Cell 2005;19:535–45.
8. Devaiah BN, Lewis BA, Cherman N, Hewitt MC, Albrecht BK, Robey PG, et al. BRD4 is an atypical kinase that phosphorylates serine2 of the RNA polymerase II carboxy-terminal domain. Proc Natl Acad Sci U S A 2012;109:6927–32.
9. LeRoy G, Rickards B, Flint SJ. The double bromodomain proteins Brd2 and Brd3 couple histone acetylation to transcription. Mol Cell 2008;30:51–60.
10. Denis GV, Vaziri C, Guo N, Faller DV. RING3 kinase transactivates promoters of cell cycle regulatory genes through E2F. Cell Growth Differ 2000;11:417–24.
11. Loven J, Hoke HA, Lin CY, Lau A, Orlando DA, Vakoc CR, et al. Selective inhibition of tumor oncogenes by disruption of super-enhancers. Cell 2013;153:320–34.
12. Filippakopoulos P, Qi J, Picaud S, Shen Y, Smith WB, Fedorov O, et al. Selective inhibition of BET bromodomains. Nature 2010;468:1067–73.
13. Mertz JA, Conery AR, Bryant BM, Sandy P, Balasubramanian S, Mele DA, et al. Targeting MYC dependence in cancer by inhibiting BET bromodomains. Proc Natl Acad Sci U S A 2011;108:16669–74.
14. Zuber J, Shi J, Wang E, Rappaport AR, Herrmann H, Sison EA, et al. RNAi screen identifies Brd4 as a therapeutic target in acute myeloid leukaemia. Nature 2011;478:524–8.
15. Delmore JE, Issa GC, Lemieux ME, Rahl PB, Shi J, Jacobs HM, et al. BET bromodomain inhibition as a therapeutic strategy to target c-Myc. Cell 2011;146:904–17.
16. Dawson MA, Prinjha RK, Dittmann A, Giotopoulos G, Bantscheff M, Chan WI, et al. Inhibition of BET recruitment to chromatin as an effective treatment for MLL-fusion leukaemia. Nature 2011;478:529–33.
17. Ott CJ, Kopp N, Bird L, Paranal RM, Qi J, Bowman T, et al. BET bromodomain inhibition targets both c-Myc and IL7R in high-risk acute lymphoblastic leukemia. Blood 2012;120:2843–52.
18. Lockwood WW, Zejnullahu K, Bradner JE, Varmus H. Sensitivity of human lung adenocarcinoma cell lines to targeted inhibition of BET epigenetic signaling proteins. Proc Natl Acad Sci U S A 2012;109:19408–13.
19. French CA, Rahman S, Walsh EM, Kuhnle S, Grayson AR, Lemieux ME, et al. NSD3-NUT fusion oncoprotein in NUT midline carcinoma: implications for a novel oncogenic mechanism. Cancer Discov 2014;4:928–41.
20. Puissant A, Frumm SM, Alexe G, Bassil CF, Qi J, Chanthery YH, et al. Targeting MYCN in neuroblastoma by BET bromodomain inhibition. Cancer Discov 2013;3:308–23.
21. Ceribelli M, Kelly PN, Shaffer AL, Wright GW, Xiao W, Yang Y, et al. Blockade of oncogenic IkappaB kinase activity in diffuse large B-cell lymphoma by bromodomain and extraterminal domain protein inhibitors. Proc Natl Acad Sci U S A 2014;111:11365–70.
22. Asangani IA, Dommeti VL, Wang X, Malik R, Cieslik M, Yang R, et al. Therapeutic targeting of BET bromodomain proteins in castration-resistant prostate cancer. Nature 2014;510:278–82.
23. Shu S, Lin CY, He HH, Witwicki RM, Tabassum DP, Roberts JM, et al. Response and resistance to BET bromodomain inhibitors in triple-negative breast cancer. Nature 2016;529:413–7.

24. Nagarajan S, Hossan T, Alawi M, Najafova Z, Indenbirken D, Bedi U, et al. Bromodomain protein BRD4 is required for estrogen receptor-dependent enhancer activation and gene transcription. Cell Rep 2014;8:460–9.
25. Amorim S, Stathis A, Gleeson M, Iyengar S, Magarotto V, Leleu X, et al. Bromodomain inhibitor OTX015 in patients with lymphoma or multiple myeloma: a dose-escalation, open-label, pharmacokinetic, phase 1 study. Lancet Haematol 2016;3:e196–204.
26. Berthon C, Raffoux E, Thomas X, Vey N, Gomez-Roca C, Yee K, et al. Bromodomain inhibitor OTX015 in patients with acute leukaemia: a dose-escalation, phase 1 study. Lancet Haematol 2016;3:e186–95.
27. Stathis A, Zucca E, Bekradda M, Gomez-Roca C, Delord JP, de La Motte Rouge T, et al. Clinical response of carcinomas harboring the BRD4-NUT oncoprotein to the targeted bromodomain inhibitor OTX015/MK-8628. Cancer Discov 2016;6:492–500.
28. Wang L, Pratt JK, McDaniel KF, Dai Y, Fidanze SD, Hasvold L, et al. Bromodomain inhibitors. Abbvie Inc.; 2014.
29. Shi J, Whyte WA, Zepeda-Mendoza CJ, Milazzo JP, Shen C, Roe JS, et al. Role of SWI/SNF in acute leukemia maintenance and enhancer-mediated Myc regulation. Genes Dev 2013;27:2648–62.
30. Zhang G, Liu R, Zhong Y, Plotnikov AN, Zhang W, Zeng L, et al. Down-regulation of NF-kappaB transcriptional activity in HIV-associated kidney disease by BRD4 inhibition. J Biol Chem 2012;287:28840–51.
31. Souers AJ, Leverson JD, Boghaert ER, Ackler SL, Catron ND, Chen J, et al. ABT-199, a potent and selective BCL-2 inhibitor, achieves antitumor activity while sparing platelets. Nat Med 2013;19:202–8.
32. Boi M, Gaudio E, Bonetti P, Kwee I, Bernasconi E, Tarantelli C, et al. The BET bromodomain inhibitor OTX015 affects pathogenetic pathways in preclinical B-cell tumor models and synergizes with targeted drugs. Clin Cancer Res 2015;21:1628–1638.
33. Noel JK, Iwata K, Ooike S, Sugahara K, Nakamura H, Daibata M. Abstract C244: Development of the BET bromodomain inhibitor OTX015. Mol Cancer Ther 2013;12:C244–C244.
34. Lovén J, Heather Hoke A, Charles Lin Y, Lau A, Orlando DA, Vakoc CR, et al. Selective inhibition of tumor oncogenes by disruption of super-enhancers. Cell 2013;153:320–334.
35. McCleland ML, Mesh K, Lorenzana E, Chopra VS, Segal E, Watanabe C, et al. CCAT1 is an enhancer-templated RNA that predicts BET sensitivity in colorectal cancer. J Clin Invest 2016;126:639–652.
36. Shi X, Mihaylova VT, Kuruvilla L, Chen F, Viviano S, Baldassarre M, et al. Loss of TRIM33 causes resistance to BET bromodomain inhibitors through MYC- and TGF-beta-dependent mechanisms. Proc Natl Acad Sci U S A 2016;113:E4558–66.
37. Rathert P, Roth M, Neumann T, Muerdter F, Roe JS, Muhar M, et al. Transcriptional plasticity promotes primary and acquired resistance to BET inhibition. Nature 2015;525:543–7.
38. Fong CY, Gilan O, Lam EY, Rubin AF, Ftouni S, Tyler D, et al. BET inhibitor resistance emerges from leukaemia stem cells. Nature 2015;525:538–42.
39. Huang M, Qiu Q, Xiao Y, Zeng S, Zhan M, Shi M, et al. BET bromodomain suppression inhibits VEGF-induced angiogenesis and vascular permeability by blocking VEGFR2-mediated activation of PAK1 and eNOS. Sci Rep 2016;6:23770.
40. Sodir NM, Swigart LB, Karnezis AN, Hanahan D, Evan GI, Soucek L. Endogenous Myc maintains the tumor microenvironment. Genes Dev 2011;25:907–16.